O'DONNELL, M. J., BENNETT, W. D. & WU, S. (1989). *J. Am. Chem. Soc.* **111**, 2353–2355.
O'DONNELL, M. J. & FALMAGNE, J. B. (1985). *Tetrahedron Lett.* **26**, 699–702.
POLT, R. & PETERSON, M. A. (1990). *Tetrahedron Lett.* **31**, 4985–4986.
POLT, R., PETERSON, M. A. & DEYOUNG, L. (1992). *J. Org. Chem.* **57**, 5469–5480.
ROQUES, R., BELLAN, J., ROSSI, J. C., DECLERCQ, J.-P. & GERMAIN, G. (1979) *Acta Cryst.* B**35**, 2467–2470.
SEEBACH, D., JUARISTI, E., MILLER, D. D., SCHICKLI, C. & WEBER, T. (1987). *Helv. Chim. Acta*, **70**, 237–261.
SHELDRICK, G. M. (1985). *SHELXS*86. In *Crystallographic Computing* 3, edited by G. M. SHELDRICK, C. KRÜGER & R. GODDARD, pp. 175–189. Oxford Univ. Press.
SKARZYNSKI, T. (1982). *Acta Cryst.* B**38**, 3110–3113.
SKARZYNSKI, T., DEREWENDA, Z., BRZOZOWSKI, A. M. & MLOSTON, G. (1982). *Acta Cryst.* B**38**, 3113–3115.
SZABÒ, L. Z., LI, Y. & POLT, R. (1991). *Tetrahedron Lett.* **32**, 585–588.

Acta Cryst. (1993). B**49**, 320–328

Structural Studies of Cyclohexane IV*

BY N. B. WILDING, J. CRAIN AND P. D. HATTON†

Department of Physics, The University of Edinburgh, Edinburgh EH9 3JZ, Scotland

AND G. BUSHNELL-WYE

SERC Daresbury Laboratory, Warrington WA4 4AD, England

(*Received* 20 *March* 1992; *accepted* 13 *July* 1992)

Abstract

We report an extensive neutron powder diffraction study of the high-pressure phase IV of cyclohexane-d_{12}. Using constrained Rietveld refinement we deduce approximate atomic positions for this phase which are found to be in close accord with the predictions of energy-minimization calculations. The likely relationship between the unit cell of phase IV and that of the ambient-pressure phase II is also presented. We further demonstrate, by means of an X-ray powder diffraction study of cyclohexane-h_{12}, that phase IV can be produced in a metastable state at ambient pressure by rapid quenching to 77 K from the liquid. This finding contradicts a previous report [Burns & Dacol (1984). *Solid State Commun.* **51**, 773–775] claiming that the ambient-pressure metastable phase is an orientational glass.

1. Introduction and background

Although a relatively simple organic molecular system, cyclohexane is characterized by a high degree of structural polymorphism in quite modest ranges of temperature and pressure (Schulte & Würflinger, 1987). It therefore represents an ideal system for studies of the processes governing structural polymorphism in organic molecular crystals. Indeed a thorough understanding of phase formation in such a simple system is a prerequisite for a wider elucidation of the generic factors governing structural phase changes in other (more complex) organic molecular materials. With this motivation, cyclohexane has been the subject of a number of detailed structural investigations.

The bulk of previous structural studies has concentrated solely on the phases obtainable at *ambient* pressure. Under these conditions, cyclohexane is known to exhibit two stable solid phases. Phase I, the plastic phase, lies between 186.1 K and the melting point at 279.82 K. It is cubic [$a = 8.61$ (2) Å; $Z = 4$; space group $Fm3m$] and from NMR studies is known to be characterized by a large degree of dynamic molecular disorder, the molecules undergoing rapid reorientations on the lattice sites (Andrew & Eades, 1953). Below 186.1 K an order–disorder transition takes place to an orientationally ordered structure (phase II). Single-crystal X-ray diffraction measurements performed by Kahn, Fourme, André & Renaud (1973) have shown that phase II possesses a monoclinic unit cell [$a = 11.23$ (2), $b = 6.44$ (2), $c = 8.20$ (2) Å, $\beta = 108.83°$; $Z = 4$; space group $C2/c$]. In the same work, a determination of the molecular positions and atomic coordinates also revealed that the molecules have the so-called 'chair-like' conformation.

In addition to the stable ambient-pressure phases, cyclohexane is also known to exhibit a *metastable* phase. This phase was discovered by Renaud &

* Neutron diffraction measurements were carried out at the Institut Laue–Langevin, Grenoble, France. X-ray diffraction measurements were carried out under the auspices of the Powder Diffraction Service, SERC Daresbury Laboratory.

† Author to whom correspondence should be addressed.

0108-7681/93/020320-09$06.00

Fourme (1966) and can be formed by rapidly quenching to low temperature from either the liquid or the plastic phase I. Using X-ray powder diffraction, these workers demonstrated that the metastable phase differs structurally from phases I and II, although the low resolution of their measurements precluded a structural determination. More recently however, (and in apparent contradiction of the X-ray work), Burns & Dacol (1984) have suggested on the basis of Raman spectroscopy measurements that the metastable phase is actually a quenched orientational glass deriving directly from phase I by the 'freezing-out' of orientational molecular disorder.

In contrast to the ambient-pressure phases of cyclohexane there is a comparative dearth of information concerning the effects of *pressure* on the adopted structures. In response to this, a number of groups have recently focused their attention on the high-pressure phases with the provisional goal of mapping the phase diagram and determining crystallographic properties as a function of pressure and temperature. These high-pressure studies have employed differential thermal analysis, vibrational spectroscopy and neutron diffraction techniques. Their principal findings are summarized below.

Three stable high-pressure phases of cyclohexane are thus far known to exist. At room temperature, all occur in the pressure range 5–18 kbar and in order of increasing pressure are denoted III, IV and V (Crain, Poon, Cairns-Smith & Hatton, 1992). Rather intriguingly, however, the transition pressures of these phases are profoundly influenced by isotopic effects, there being dramatic differences between C_6H_{12} and its deuterated derivative C_6D_{12}. For example, at room temperature, the phase III–IV transition in C_6D_{12} is observed at a pressure of 7.4 kbar, while in C_6H_{12} the same transition occurs at the considerably higher pressure of 9.6 kbar (Haines & Gilson, 1989, 1990).

Using differential thermal analysis (DTA), Schulte & Würflinger (1987) have mapped the phase diagrams of C_6H_{12} and C_6D_{12} (and mixtures thereof) both as a function of pressure (to 3 kbar) and temperature. The resulting picture of the phase diagram for both isotopic forms was subsequently complemented by room-temperature Raman and infrared vibrational spectroscopy measurements as a function of pressure (Haines & Gilson, 1989, 1990). This latter work gave some indications regarding the point-group symmetry of the high-pressure phases III and IV. Moreover, the observed transition pressures allowed an extrapolation to higher pressures of the DTA-based phase diagram.

Figs. 1(*a*) and 1(*b*) show the extrapolated phase diagrams of Schulte & Würflinger (1987) for C_6H_{12} and C_6D_{12} respectively. The influence of the isotope effect is striking, particularly with regard to phase IV. Although this phase is observed at low temperatures in C_6D_{12} for pressures between 1.5 and 3 kbar, no direct evidence for its presence at low temperature was seen in C_6H_{12} up to 3 kbar (the pressure limit of the DTA study). Nevertheless the DTA work on mixtures of C_6D_{12} and C_6H_{12} suggests that phase IV could exist in pure C_6H_{12}, but that the triple point of phases II, III and IV would be shifted to pressures above 3 kbar. Indeed this proposal is consistent with recent room-temperature Raman spectroscopy measurements performed by Crain *et al.* (1992) which demonstrate that phase IV does occur in C_6H_{12} for pressures above approximately 10 kbar. Thus there would appear to be nothing to suggest that deuteration engenders any fundamental topological change in the phase diagram of cyclohexane.

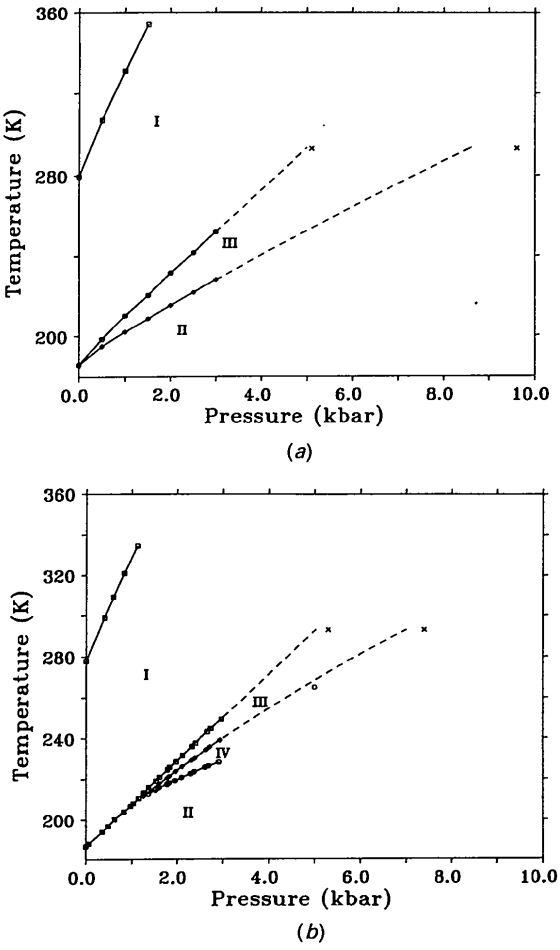

Fig. 1. The extrapolated phase diagrams of Schulte & Würflinger (1987) for (*a*) C_6H_{12} and (*b*) C_6D_{12}. The broken lines represent the extrapolation to room temperature of a polynomial fit to the DTA data. The points (×) at 293 K correspond to the boundary of phase III as determined by Haines & Gilson (1989, 1990). The point (○) at 5 kbar, 265 K indicates the position of the phase III–IV boundary determined by Wilding *et al.* (1991).

In addition to the effects of deuteration, studies of the phase diagram of cyclohexane are further complicated by pronounced metastability effects. In particular, [and as recently detailed by Mayer *et al.* (1991) for C_6D_{12}], there are regions of the phase diagram where phase IV manifests a remarkable degree of metastability with respect to the stable low-temperature ambient-pressure phase II (*cf.* Fig. 1*b*). Mayer *et al.* (1991) noted that the position of the phase IV–II boundary is strongly dependent on the direction in which it is traversed and that the locus of this boundary, as recorded in Fig. 1, strictly only applies when heating from phase II. On cooling from phase IV at 3 kbar, they found that phase IV could be supercooled (with respect to Fig. 1*b*) at least as low as 175 K (the lower temperature limit of their study).

Although no structural information has yet been deduced for the recently discovered phase V, detailed structural information on phases III and IV has recently been published by Wilding, Hatton & Pawley (1991). These authors performed a high-pressure neutron powder diffraction study and successfully determined the unit cell and space group of both phases. Phase III was found to be orthorhombic [$a = 6.587$ (3), $b = 7.844$ (7), $c = 5.295$ (3) Å, $Z = 2$] with space group *Pmnn*. The unit cell and space group of phase IV were found to be closely related to those of phase III; it is monoclinic [$a = 6.526$ (4), $b = 7.597$ (6), $c = 5.463$ (5) Å, $\beta = 97.108$ (4)°, $Z = 2$], with space group $P12_1/n1$. In addition, approximate atomic positions were determined for phase III using lattice-energy minimization techniques in conjunction with constrained Rietveld refinement. This showed that in common with phase II, the molecule in phase III adopts the 'chair' conformation. Unfortunately, no reliable conclusions were obtained regarding the atomic positions in phase IV.

Evidently a full structural solution of phase IV remains one of the major outstanding structural problems posed by cyclohexane. Without knowledge of this structure, the mechanism of the phase IV–II transition (and hence the underlying cause of the metastability effect) cannot be deduced. In view of this, we now revisit phase IV with the aim of determining the atomic positions and investigating further the extent of its metastability with respect to phase II.

2. Experimental and results

2.1. *Neutron powder diffraction studies of* C_6D_{12} *at high pressure*

Data were collected using the high-resolution D2B neutron diffractometer at the Institut Laue–Langevin (ILL) (Hewat & Bailey, 1976). An incident neutron wavelength of 1.5938 ± 0.0002 Å was used and calibrated using a silicon wavelength standard. For high-pressure measurements at low temperatures, a 6 kbar helium pressure cell was employed in conjunction with a standard orange cryostat. The pressure, as indicated by the calibration of the pumping apparatus, was independently corroborated by a strain-gauge instrument accurate to better than 0.1 kbar. The aluminium housing of the pressure cell gave rise to diffraction peaks 111, 200, 222 and 311 centred at 39.9, 46.0, 67.2 and 81.7° of 2θ respectively. Those reflections lying in the immediate vicinity of these non-sample reflections were excluded from the set used for the refinement procedure.

A commercially available sample of C_6D_{12} with a stated deuterium purity of 99.5% was obtained from the Aldrich chemical company. The sample was introduced in liquid form to the sample holder, a 12 mm diameter vanadium can. In an attempt to ensure homogeneity of the powder, the sample can was packed with silica wool prior to introduction of the sample. Scattering from the silica wool itself is known to add uniformly to the background and thus had negligible effect on the sample pattern (Baharie & Pawley, 1977).

At a pressure of 5 kbar, the sample was cooled from room temperature to 250 K. A short scan at this temperature yielded a powder pattern consistent with the known unit-cell parameters of phase IV, as previously determined by Wilding *et al.* (1991). A high-quality data set suitable for structure determination was then collected over a period of 4 h, yielding data in the 2θ range 0–120° with a 2θ step size of 0.05°. Holding the pressure at 5 kbar, the temperature was then slowly reduced to 60 K in an attempt to locate any transition to phase II. However, none was observed even though the sample was held at 5 kbar, 60 K for several hours. Maintaining the temperature constant at 60 K, the pressure was then reduced stepwise from 5 kbar to ambient pressure (1 bar). At each pressure a short data set of 30 min duration was collected. Somewhat surprisingly, phase IV was found to persist right down to 1 bar. Only by heating the sample at ambient pressure was a transition from phase IV to phase II finally induced at approximately 160 K.

The short data sets collected at each pressure were used to obtain estimates of the phase IV unit-cell parameters. The peak positions of the Bragg reflections were input to the *CELREF* program (Fitch & Murray, 1992), which produced a least-squares estimate for the lattice parameters. These parameters (normalized with respect to their ambient-pressure values), are presented in Fig. 2. From this figure it is clear that the unit cell is considerably more compressible along the [010] direction than along either the [100] or [001] directions.

In order to deduce the atomic positions of the phase IV structure, the high-quality data set collected at 5 kbar, 250 K was analysed using the *EDINP* constrained Rietveld refinement program (Pawley, 1980). Prior to refinement, the unit-cell parameters, zero error and peak-shape function were first fitted using the *ALLHKL* profile refinement program (Pawley, 1981). The resulting estimates for instrumental and unit-cell parameters fitted in the 2θ range 15–120° are given in Table 1 and were used subsequently in the Rietveld refinement.

An 'idealized' chair-shaped cyclohexane molecule was used for the Rietveld refinement. This molecule has tetrahedral bond angles with bond lengths C—C = 1.53 and C—D = 1.07 Å. Strict constraints were applied to the molecule to ensure that the bond lengths and bond angles remained constant – only the orientation of the molecule was permitted to vary. The refinement was performed subject to the $P12_1/n1$ space group with $Z = 2$, as previously determined by Wilding *et al.* (1991). This space group dictates that the centre of one molecule coincides with the unit-cell corner, while the centre of the other molecule lies at the cell centre. Since the unit cells of phases III and IV are both very similar to one another in size and shape, the initial molecular orientation for the phase IV refinement was chosen to be approximately the same (relative to a fixed Cartesian basis) as that for the known phase III. The powder pattern was refined in the 2θ range 15–120° and only four parameters were varied: the scale factor of the pattern and the three Euler angles controlling the molecular orientation. Isotropic temperature factors were not refined, and were set to 1.11 for the C atoms and 5.53 for the D atoms. The background took the form of a linear interpolation between visually estimated points.

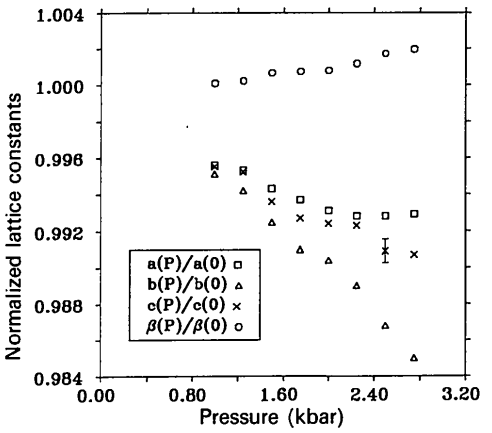

Fig. 2. The pressure dependence of the unit-cell parameters of C_6D_{12} at 60 K. The data are normalized with respect to the ambient-pressure cell constants $a = 6.586$, $b = 7.582$, $c = 5.557$ Å, $\beta = 98.064°$. A typical error bar is also shown.

Table 1. *Values from the ALLHKL program for the instrumental and lattice parameters of phase IV in* C_6D_{12} *at* 5 kbar, 250 K

Zero (°)	−0.338 (2)
u (deg^2)	0.709 (1)
v (deg^2)	−0.728 (8)
w (deg^2)	0.324 (1)
a (Å)	6.529 (4)
b (Å)	7.601 (7)
c (Å)	5.461 (6)
β (°)	96.97 (1)
Volume (Å^3)	269.07 (4)

The refinement converged rapidly with final R factors of $R_I = 14.0$, $R_{wp} = 19.65$, $R_{exp} = 2.87\%$ where we have used:

$$R_I = \{\Sigma[|I(\text{obs}) - I(\text{calc})|]/\Sigma[I(\text{obs})]\} \times 100\%,$$

$$R_{wp} = (\Sigma\{w[Y(\text{obs}) - Y(\text{calc})]^2\}/\Sigma[wY(\text{obs})^2])^{1/2} \times 100\%,$$

$$R_{exp} = [(N - P + C)/\Sigma\{w[Y(\text{obs})]^2\}]^{1/2} \times 100\%.$$

Here N is the number of data points, P is the number of parameters and C is the number of constraint functions. Also $Y(\text{obs}) = Y(\text{total}) - \text{background}$, $w = 1/[Y(\text{total}) + \text{background}]$.

A difference plot of the refined pattern is shown in Fig. 3.* In the interests of clarity the pattern has been truncated to show only the portion of the scan between 15 and 80° of 2θ. The atomic positions for this solution are given in Table 2 and a carbon skeletal representation of the molecular orientation is shown in Fig. 4. Notwithstanding the rather large R factors, there are a number of reasons why we believe that this structure is essentially correct.

Firstly, the origin of the large R factors can be traced to inadequate powder averaging. Comparison of the powder pattern shown in Fig. 3 with that obtained previously under the same conditions [Fig. 2*b* of Wilding *et al.* (1991)] reveals significant discrepancies between the relative intensities of the Bragg peaks. We interpret this irreproducibility as arising from powder inhomogeneities, implying that the silica wool is not entirely effective in producing a fine powder. Although the magnitude of the effect is sufficient to account for the unexpectedly large R factor, it is not (we believe) so great that the solution can be discounted as unreliable. Indeed, trial refinements with many different starting orientations *always* refined to the solution depicted in Fig. 4, giving more confidence that the solution is substantially correct.

Secondly, inspection of Fig. 4 shows that the molecular orientation in phase IV is closely related

* Primary diffraction data corresponding to Figs. 3 and 5 have been deposited with the British Library Document Supply Centre as Supplementary Publication No. SUP 55955 (18 pp.). Copies may be obtained through The Technical Editor, International Union of Crystallography, 5 Abbey Square, Chester CH1 2HU, England.

Table 2. *Refined atomic positions in phase IV at 5 kbar, 250 K based on a constrained molecular geometry*

Only half the atoms per molecule are given, the remainder follow from an inversion through the origin. The estimated standard deviations on the Euler angles φ, θ and ψ which control the molecular orientation are 0.017, 0.016 and 0.018° respectively.

	x	y	z
C1	0.203	−0.068	0.102
C2	0.172	0.028	−0.147
C3	−0.002	0.163	−0.145
D1	0.242	0.025	0.248
D2	0.133	−0.065	−0.292
D3	0.037	0.257	0.001
D4	0.325	−0.163	0.101
D5	0.312	0.094	−0.176
D6	−0.024	0.231	−0.319

to that of phase III [Fig. 6 of Wilding *et al.* (1991)]. This is just as one might anticipate given the close relationship between the unit cell and space group of phases III and IV. The main qualitative feature of the transition is a rotation of the molecule in the same sense as the monoclinic distortion, thereby ensuring that the C3 atom remains in the (001) plane. There is also a small (~7°) rotation of the molecule about the axis in the (001) plane which joins the origin to the C3 atom.

Thirdly, the deduced structure of phase IV is in excellent agreement with that predicted by the energy-minimization calculations of Wilding *et al.* (1991) and given in Table 3. Without prior knowledge of the powder averaging problem, these workers discounted their energy-minimization results because a corresponding high-quality Rietveld refinement of their phase IV powder pattern could not be obtained.

The remainder of our evidence supporting the proposed structure of phase IV derives from a separate X-ray powder diffraction study of the ambient-pressure metastable phase of cyclohexane. Details of this study are described in the following subsection.

2.2 *X-ray diffraction studies of the ambient-pressure metastable phase in* C_6H_{12}

Low-temperature powder X-ray diffraction measurements were performed on Station 9.1 of the Daresbury Synchrotron Radiation Source (SRS) using 1.004 Å radiation from a 3-pole, 5 T Wiggler magnet and a channel-cut Si(111) monochromator. A commercially available sample of C_6H_{12} with a stated purity of 99.5% was obtained from the Aldrich chemical company and loaded in the liquid state into a 0.3 mm glass capillary which was subsequently sealed at both ends. This capillary was then quenched to 77 K in liquid nitrogen and quickly loaded into a pre-cooled cryostat. Both the quenching and loading were carried out under a nitrogen atmosphere in order to limit moisture condensation onto the capillary. The cryostat was an Oxford Instruments continuous-flow type (model CF1238), having the capability to rotate the sample during data collection for improved powder averaging. At 77 K, temperature stability was found to be better than ± 1 K.

A powder pattern of the quenched sample was collected at 77 K, in the 2θ range 3–30° for a 2θ step size of 0.01°. Examination of this pattern revealed it to comprise a mixture of both phases IV and II in respective proportions of approximately 8:1. Consequently we conclude that the metastable phase dis-

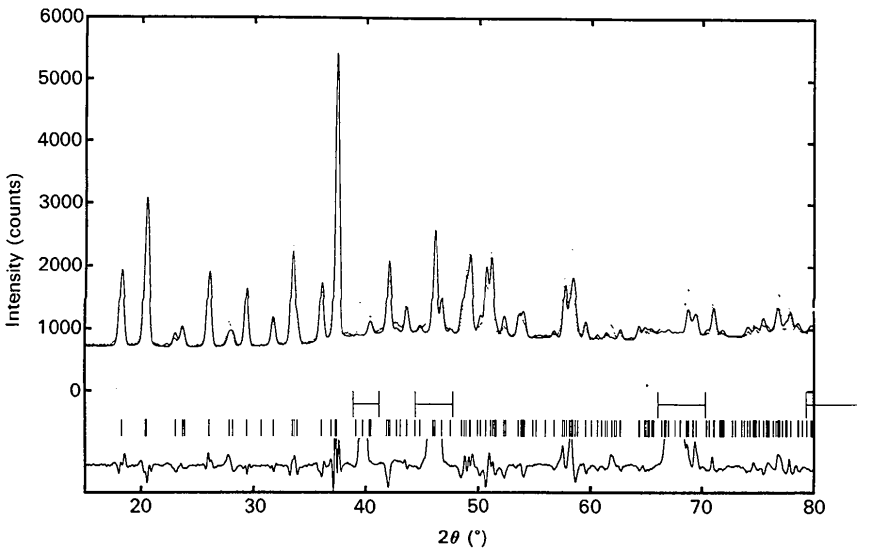

Fig. 3. A portion of the difference plot of the refined phase IV pattern at 5 kbar, 250 K. The horizontal bars signify those portions of the pattern which were excluded from the refinement.

covered by Renaud & Fourme (1966) is none other than phase IV. Indeed the *d* spacings of the phase IV structure are consistent with the X-ray powder diffraction data of Renaud & Fourme (1966), despite the low resolution of their study. Futhermore these workers also on occasion observed a mixture of phases following a quench – an effect they ascribed to an insufficient cooling rate.

The peak positions for both constituent phases, together with their indexing assignments and intensities are given in Table 4. Owing to the presence of a mixture of phases II and IV, it was necessary to employ multiphase Rietveld refinement to analyse the powder pattern of the quenched sample. This was achieved using the *MPROF* program available at Daresbury (Fitch & Murray, 1992). The atomic positions for the phase II component were taken from the data of Kahn *et al.* (1973), while those for the phase IV component were taken from Table 2. Isotropic temperature factors for the C and H atoms were not refined and were set to 1.11 and 7.03 respectively. The background was input in the form of visually estimated points with intermediate points being obtained by linear interpolation. Chemical (slack) constraints were placed on the bond angles and bond lengths. These favoured C=C and C=H bond lengths of 1.53 and 1.07 Å respectively. Bond angles were set to favour the tetrahedral symmetry of approximately 110°. The refinement proceeded normally, yielding final *R* factors of $R_I = 7.88$, $R_{wp} = 18.84$, $R_{exp} = 14.38\%$ for 43 refined parameters. A difference plot of the refined pattern is given in Fig. 5. Refined values of the instrumental parameters, lattice parameters and atom positions appear in Tables 5, 6 and 7 respectively.

Comparison of Tables 2 and 7 shows that the atom positions in the metastable phase IV in C_6H_{12} are in good general agreement with those deduced for the stable phase IV in C_6D_{12} from high-pressure neutron diffraction experiments, notwithstanding the differences in isotopic form and temperature and pressure between both experiments. Such agreement between both X-ray and neutron measurements represents perhaps the single most exacting test of a structure solution. As such, it constitutes substantial corroboration of the structure solution advanced here.

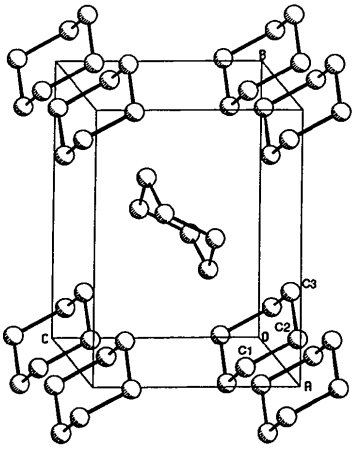

Fig. 4. A carbon skeletal representation of the refined structure of phase IV obtained from the constrained Rietveld refinement of the neutron powder pattern at 5 kbar, 250 K.

Table 3. *Atomic positions in phase IV as predicted by the energy-minimization calculations of Wilding et al.* (1991)

	x	*y*	*z*
C1	0.2061	−0.0720	0.1034
C2	0.1712	0.0226	−0.1518
C3	−0.0024	0.1646	−0.1524
D1	0.2468	0.0158	0.2322
D2	0.1304	−0.0653	−0.2807
D3	0.0383	0.2524	−0.0236
D4	0.3150	−0.1611	0.1038
D5	0.2990	0.0806	−0.1826
D6	−0.0243	0.2239	−0.3125

Table 4. *Observed and calculated reflections of* C_6H_{12} *at* 1 bar, 77 K *following a quench from room temperature*

The pattern comprises a mixture of phases II and IV. The calculated reflections ($2\theta_{calc}$) were generated using the refined cell parameters and zero error given in Table 5. The pattern also contains two unidentified contaminant peaks at low angle which possibly arise from ice on the sample capillary.

2θ (°)	Count	$2\theta_{calc}$ (°)	Phase	*hkl*	$\Delta 2\theta$ (°)
10.729	2082	10.734	II	2 0 0	0.005
11.103	1820	Contaminant			
11.534	7750	11.529	IV	1 1 0	−0.005
11.764	2500	11.766	II	−1 1 1	0.002
12.217	1489	Contaminant			
12.641	2169	12.640	IV	−1 0 1	−0.001
12.828	8971	12.831	IV	0 1 1	0.003
13.798	1349	13.792	II	1 1 1	−0.006
14.467	2326	14.466	IV	1 0 1	−0.001
14.740	1489	14.729	IV	−1 1 1	−0.011
14.884	1506	14.880	II	0 0 2	−0.004
15.082	1451	15.077	IV	0 2 0	−0.005
15.291	1032	15.302	II	−2 0 2	0.011
16.326	2733	16.328	IV	1 1 1	0.002
16.734	779	16.726	II	−1 1 2	−0.008
17.447	797	17.456	IV	1 2 0	0.009
18.345	2079	18.350	IV	0 2 1	0.005
20.614	1227	20.612	IV	−2 1 1	−0.002
20.981	541	20.984	II	2 2 0	0.003
21.610	414	21.598	II	4 0 0	−0.012
21.843	411	21.846	II	3 1 1	0.003
22.203	882	22.218	IV	0 1 2	0.015
23.216	953	23.213	IV	2 2 0	−0.003
23.691	367	23.694	II	−2 2 2	0.003
24.388	350	24.385	IV	1 3 0	−0.003
27.048	383	27.049	IV	1 3 1	0.001
27.532	374	27.531	IV	3 1 0	−0.001
28.256	850	28.269	IV	1 2 2	0.013

3. Discussion and concluding remarks

In summary, we have employed neutron powder diffraction methods to study the structural properties

of phase IV in C_6D_{12} at high pressures. Using constrained Rietveld refinement, approximate atomic coordinates were deduced which agree well with the predictions of lattice-energy minimization calculations. The lattice parameters at 60 K were also measured as a function of decreasing pressure in the range 5 kbar down to 1 bar. This revealed the unit cell of phase IV to be considerably more compressible along the [010] vector than along either the [100] or the [001] direction. No transition from phase IV to phase II was observed at 60 K, even when the pressure was reduced to its ambient value. Additional X-ray powder diffraction measurements further demonstrated that phase IV can be produced at ambient pressure by quenching from the liquid to 77 K. Although this latter finding is consistent with the X-ray diffraction data of Renaud & Fourme (1966), it is at variance with the assertion of Burns & Dacol (1984) that the ambient-pressure metastable phase is a 'plastic crystal glass'.

Addressing now the general issues raised by these findings, we have shown that phase IV can exist at ambient pressures provided it is prepared in either of two ways. One technique is first to form phase IV at high pressures and then, provided the temperature is maintained sufficiently low,* no transformation to the stable phase II will occur when the pressure is released. Alternatively one can produce phase IV directly at ambient pressure by quenching in liquid nitrogen from either the liquid or phase I. Again for this to succeed, the final temperature must be sufficiently low to prevent a subsequent transition to phase II.

In our view, both these findings manifest two basic characteristics of phases II and IV, namely that at ambient pressure they possess comparable lattice energies but are separated from one another by a large energy barrier. The first of these assertions is evidenced by the almost identical molecular volume in both the coexisting phases, *cf.* Table 6. The second derives from an examination of what we regard as the most likely relationship between the unit cells of phases II and IV. This relationship is displayed schematically in Fig. 6. It shows those intermolecular vectors in the phase II unit cell that correspond to the lattice vectors of the phase IV cell. The matrix relating vectors in the basis of the assumed phase IV unit cell to those of the phase II cell is given below.

$$\begin{pmatrix} x/a' \\ y/b' \\ z/c' \end{pmatrix}_{II} = \begin{pmatrix} \frac{3}{4} \\ \frac{3}{4} \\ 0 \end{pmatrix} + \begin{pmatrix} 0 & -\frac{1}{2} & -\frac{1}{2} \\ -1 & 0 & 0 \\ 0 & \frac{1}{2} & -\frac{1}{2} \end{pmatrix} \begin{pmatrix} x/a \\ y/b \\ z/c \end{pmatrix}_{IV}$$

where the notation is defined in Fig. 6 and the origin of cell IV is translated by $(3a'/4, 3b'/4, 0)$ with respect to that of phase II.

The lengths of the phase IV lattice vectors calculated on the basis of the *measured* phase II cell are given in the figure. They are consistent to within 4% with the measured phase IV lattice vectors (Table 6). However, significant differences exist for the intermolecular angles. Principally, we find that in order to effect the transition, the angle α of the phase IV cell must decrease substantially from 90 to 77.25°, while

* Wilding *et al.* (1991) observed the phase IV–II transition at 2 kbar, 175 K for decreasing pressure.

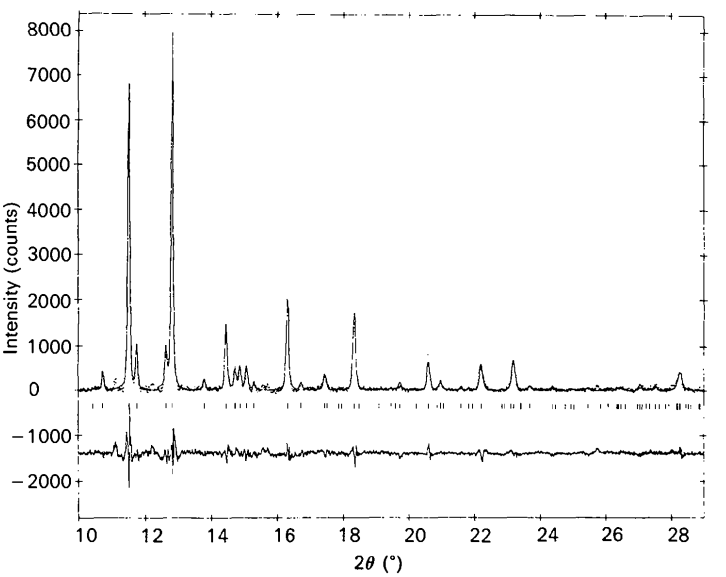

Fig. 5. Difference plot of the Rietveld refinement of the X-ray powder pattern of the quenched sample of C_6H_{12} at 77 K. The pattern contains contributions from phases IV and II in respective proportions of approximately 8:1.

Table 5. *Refined values of the principal instrumental parameters for the quenched sample of* C_6H_{12} *at* 1 bar, 77 K

2θ refinement range (°)	10–35
Scale (IV)	0.234 (2)
Scale (II)	0.032 (1)
Zero (°)	−0.034 (2)
u (deg^2)	−0.4166 (4)
v (deg^2)	0.2105 (2)
w (deg^2)	−0.0128 (1)

Table 6. *Refined lattice parameters in phases II and IV for the quenched sample of* C_6H_{12} *at* 1 bar, 77 K

Parameter	Phase IV	Phase II
a (Å)	6.637 (8)	11.302 (7)
b (Å)	7.635 (2)	6.419 (1)
c (Å)	5.585 (6)	8.172 (5)
β (°)	97.77 (8)	108.78 (7)
Volume (Å^3)	280.4	561.3

Table 7. *Refined atomic positions in phases II and IV for the quenched sample of* C_6H_{12} *at* 1 bar, 77 K

	Phase	x	y	z
C1	IV	0.209 (1)	−0.080 (5)	0.066 (4)
C2	IV	0.161 (2)	0.032 (2)	−0.164 (3)
C3	IV	−0.018 (2)	0.157 (2)	−0.156 (5)
H1	IV	0.266 (8)	0.001 (4)	0.214 (5)
H2	IV	0.175 (7)	−0.044 (2)	−0.320 (5)
H3	IV	0.003 (8)	0.229 (7)	0.009 (6)
H4	IV	0.321 (8)	−0.177 (9)	0.038 (8)
H5	IV	0.263 (9)	0.142 (6)	−0.153 (6)
H6	IV	−0.031 (8)	0.244 (9)	−0.309 (6)
C1	II	0.211 (2)	0.461 (3)	0.019 (2)
C2	II	0.351 (2)	0.400 (4)	0.102 (2)
C3	II	0.379 (1)	0.221 (5)	−0.014 (3)
H1	II	0.195 (6)	0.530 (2)	0.893 (7)
H2	II	0.142 (6)	0.684 (4)	0.190 (8)
H3	II	0.391 (8)	0.355 (5)	0.349 (5)
H4	II	0.413 (4)	0.524 (5)	0.078 (8)
H5	II	0.317 (6)	0.282 (6)	0.774 (6)
H6	II	0.488 (4)	0.211 (3)	0.020 (9)

the value of β must decrease from 97.767 to 90°. As the packing in the two phases is clearly quite distinct, [*cf.* Fig. 4 of this work and Fig. 2 of Kahn *et al.* (1973)], the transition will require considerable molecular reorganization – a process that will be opposed by the steric hindrance of the molecules themselves. It is therefore not too surprising that the phase IV–II transition is absent at low temperatures.

To understand thoroughly the formation of phase IV in preference to phase II on rapid cooling requires information on the detailed dynamics of the molecular ordering processes. Unfortunately, the degree of dynamical information available from a structural study such as ours is very limited. Thus it is difficult to speculate confidently on the ordering mechanisms which take place during the quench. However, some insight is again furnished by a consideration of the molecular packing arrangements in phases IV and II. From Fig. 4 it is clear that the molecules in phase IV pack in a 'herringbone' fashion. However in phase II, the packing is somewhat more complex [Fig. 2 of Kahn *et al.* (1973)]. It is therefore likely that the formation of phase II requires considerably more cooperative behaviour among neighbouring molecules than does phase IV. Given insufficient opportunity for such cooperation, as is the case during a quench, it is not unreasonable that the system will adopt preferentially the less-stable phase IV structure.

Our neutron powder diffraction patterns provide reliable information concerning the lattice parameters and approximate molecular orientation of phase IV at high pressure. However, accurate values for intramolecular bond angles and bond lengths could not be obtained because of the powder averaging problem.* Thus we have no direct indication of whether pressure-induced molecular distortion plays a significant role in the high-pressure phase transformations. Nevertheless, the fact that the atomic positions in both phases III and IV were correctly

* Indeed this effect may go some way to explaining the rather distorted molecular geometry found previously by Wilding *et al.* (1991) in similar neutron powder diffraction studies of phase III.

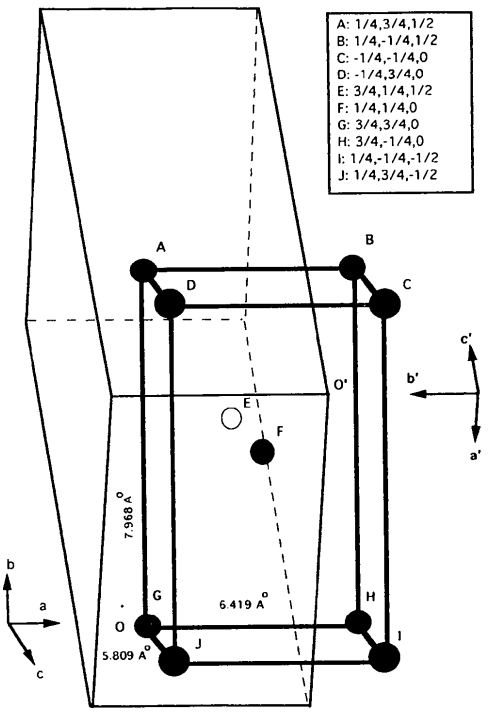

Fig. 6. A schematic view of the relationship between phases II and IV showing the positions of the molecular centres. The inset gives the fractional positions of each molecular centre in the phase II basis. The marked distances are the lengths of those intermolecular vectors in the measured phase II unit cell which transform to become lattice vectors of the phase IV cell. The origins of the phase IV and phase II cells are marked as O and O' respectively.

identified by *rigid-molecule* energy-minimization calculations, itself suggests that distortion effects are likely to be small. In conclusion, therefore, we believe that the combined use of powder diffraction and energy minimization represents a powerful technique for structure solution in organic molecular systems. In future work we intend to extend their use to studies of related materials such as cyclohexanol and cyclohexanone.

We would like to express our thanks to Dr A. W. Hewat, Mr John Davies and Mr A. M. T. Bell for their expert assistance during the experiments. We have also benefitted from helpful discussions with G. S. Pawley. This work was funded in part by the SERC through access to research facilities at the Institut Laue–Langevin and Daresbury Laboratory.

References

ANDREW, E. R. & EADES, R. G. (1953). *Proc. R. Soc. London Ser. A*, **216**, 398–412.

BAHARIE, E. & PAWLEY, G. S. (1977). *J. Appl. Cryst.* **10**, 465–467.

BURNS, G. & DACOL, F. H. (1984). *Solid State Commun.* **51**, 773–775.

CRAIN, J., POON, W. C.-K., CAIRNS-SMITH, A. & HATTON, P. D. (1992). *J. Phys. Chem.* **96**, 8168–8173.

FITCH, A. N. & MURRAY, A. D. (1992). *PDPL*. An integrated powder diffraction program library. In preparation.

HAINES, J. & GILSON, D. F. R. (1989). *J. Phys. Chem.* 7920–7925.

HAINES, J. & GILSON, D. F. R. (1990). *J. Phys. Chem.* **94**, 4712–4716.

HEWAT, A. W. & BAILEY, I. (1976). *Nucl. Instrum. Methods*, **137**, 463.

KAHN, R., FOURME, R., ANDRÉ, D. & RENAUD, M. (1973). *Acta Cryst.* B**29**, 131–138.

MAYER, J., URBAN, S., HABRYLO, S., HOLDERNA, K., NATKANIEC, I., WÜRFLINGER, A. & ZAJAC, W. (1991). *Phys. Status Solidi*, B**166**, 381–394.

PAWLEY, G. S. (1980). *J. Appl. Cryst.* **13**, 630–633.

PAWLEY, G. S. (1981). *J. Appl. Cryst.* **14**, 357–361.

RENAUD, M. & FOURME, R. (1966). *J. Chim. Phys.* **62**, 27–32.

SCHULTE, L. & WÜRFLINGER, A. (1987). *J. Chem. Thermodyn.* **19**, 363–368.

WILDING, N. B., HATTON, P. D. & PAWLEY, G. S. (1991). *Acta Cryst.* B**47**, 797–806.

Acta Cryst. (1993). B**49**, 328–334

Structures of Four *N*-Benzoylaziridine and Aziridinium *p*-Toluenesulfonate Derivatives Grafted onto 7-Oxabicyclo[2.2.1]heptane Skeletons

BY A. ALAN PINKERTON,* ANTHONY C. GALLACHER, MARK RADIL AND ANDREAS KUNZE

Department of Chemistry of the University of Toledo, 2801 *W. Bancroft Street, Toledo, Ohio* 43606, *USA*

AND SUSY ALLEMANN AND PIERRE VOGEL*

Section de Chimie de l'Université de Lausanne, 2 *rue de la Barre, CH*-1005 *Lausanne, Switzerland*

(*Received* 2 *January* 1992; *accepted* 21 *July* 1992)

Abstract

Dimethyl 3-benzoyl-8-oxa-3-azatricyclo[3.2.1.$0^{2,4}$]-octane-6,7-dicarboxylate (7), $C_{17}H_{17}NO_6$, M_r = 331.33, monoclinic, $P2_1/c$, a = 5.362 (1), b = 24.558 (3), c = 11.793 (1) Å, β = 96.42 (1)°, V = 1543 (1) Å^3, Z = 4, D_x = 1.43 g cm^{-3}, λ(Mo $K\alpha$) = 0.70930 Å, μ = 1.0 cm^{-1}, $F(000)$ = 696, T = 123 (1) K, R = 0.047 for 1743 unique observed reflections. *cis*-6,7-Dimethoxycarbonyl-8-oxa-3-azoniatricyclo[3.2.1.$0^{2,4}$]octane *p*-toluenesulfonate (14), $C_{17}H_{21}NO_8S$, M_r = 399.42, monoclinic, $P2_1/c$, a = 14.160 (4), b = 5.514 (1), c = 23.792 (7) Å, β = 100.16 (2)°, V = 1828 (2) Å^3, Z = 4, D_x = 1.45 g cm^{-3}, λ(Mo $K\alpha$) = 0.70930 Å, μ = 2.1 cm^{-1}, $F(000)$ = 840, T = 193 (1) K, R = 0.045 for 2737 unique observed reflections. *trans*-6,7-Dimethoxycarbonyl-8-oxa-3-azoniatricyclo[3.2.1.$0^{2,4}$]octane *p*-toluenesulfonate (18), $C_{17}H_{21}NO_8S$, M_r = 399.42, monoclinic, $P2_1/n$, a = 21.501 (6), b = 5.476 (2), c = 15.858 (2) Å, β = 90.68 (2)°, V = 1867 (1) Å^3, Z = 4, D_x = 1.42 g cm^{-3}, λ(Mo $K\alpha$) = 0.70930 Å, μ = 2.1 cm^{-1}, $F(000)$ = 840, T = 123 (1) K, R = 0.029 for 1680 unique observed reflections. 3-Benzoyl-6-cyano-8-oxa-3-azatricyclo[3.2.1.$0^{2,4}$]oct-6-yl acetate (19), $C_{16}H_{14}N_2O_4$, M_r = 298.30, triclinic, $P\bar{1}$, a = 5.654 (1), b = 8.088 (3), c = 16.223 (7) Å, α = 103.78 (3), β = 90.35 (3), γ = 98.29 (2)°, V = 712 (1) Å^3, Z = 2, D_x = 1.39 g cm^{-3}, λ(Mo $K\alpha$) = 0.70930 Å, μ = 0.9 cm^{-1}, $F(000)$ = 312, T = 294 (1) K, R = 0.040 for 2021 unique observed reflections. The crystal structures of the aziridinium salts (14) and (18) and of the *N*-

* To whom correspondence should be addressed

0108-7681/93/020328-07$06.00